ELSEVIER

Physica A 312 (2002) 260–276

PHYSICA A

www.elsevier.com/locate/physa

Simulation of evacuation processes using a bionics-inspired cellular automaton model for pedestrian dynamics

Ansgar Kirchner *, Andreas Schadschneider

Institut für Theoretische Physik, Universität zu Köln, D-50923 Köln, Germany

Received 1 February 2002

Abstract

We present simulations of evacuation processes using a recently introduced cellular automaton model for pedestrian dynamics. This model applies a bionics approach to describe the interaction between the pedestrians using ideas from chemotaxis. Here we study a rather simple situation, namely the evacuation from a large room with one or two doors. It is shown that the variation of the model parameters allows to describe different types of behaviour, from regular to panic. We find a non-monotonic dependence of the evacuation times on the coupling constants. These times depend on the strength of the herding behaviour, with minimal evacuation times for some intermediate values of the couplings, i.e., a proper combination of herding and use of knowledge about the shortest way to the exit. © 2002 Published by Elsevier Science B.V.

PACS: 45.70.Vn; 89.40.+k; 89.65.Lm; 05.65.+b

Keywords: Cellular automata; Non-equilibrium physics; Pedestrian dynamics

1. Introduction

Methods from physics have been successfully used for the investigation of vehicular traffic for a long time [1,2]. On the other hand, pedestrian dynamics has not been studied as extensively [3]. Due to its generically two-dimensional nature, pedestrian motion is more difficult to describe in terms of simple models. However, many interesting collective effects and self-organisation phenomena have been observed (see Refs. [2,4] for an overview and a comprehensive list of references), e.g. jamming and clogging,

* Corresponding author.
E-mail addresses: aki@thp.uni-koeln.de (A. Kirchner), as@thp.uni-koeln.de (A. Schadschneider).

0378-4371/02/$ - see front matter © 2002 Published by Elsevier Science B.V.
PII: S0378-4371(02)00857-9

lane formation and oscillations at bottlenecks in counterflow or collective patterns of motion at intersections. These phenomena will be discussed in Section 2.4.

The model takes its inspiration[1] from the process of chemotaxis (see Ref. [5] for a review). Some insects create a chemical trace to guide other individuals to food places. This is also the central idea of the active-walker models used for the simulation of trail formation. In the approach of [6] the pedestrians also create a trace. In contrast to trail formation and chemotaxis, however, this trace is only virtual although one could assume that it corresponds to some abstract representation of the path in the mind of the pedestrians. Its main purpose is to transform effects of long-ranged interactions (e.g. following people walking some distance ahead) into a local interaction (with the "trace"). This allows for a much more efficient simulation on a computer.

The basic idea of our approach might be used for studying a variety of problems, especially from biology [6–8]. Here we want to apply this model to a simple evacuation process with people trying to escape from a large room. Such a situation can lead to a panic where individuals apparently act irrationally. A nice discussion of empirical results can be found in Ref. [4]. Our motivation here is rather the determination and classification of the different types of behaviour exhibited by the model than a realistic application.

The phenomena observed during panics can be quite different from those found in "normal" situations. Nevertheless, it is desirable to have a model which is able to describe the whole spectrum of possible pedestrian behaviour in a unified way. So far mainly the social-force model [9] has been used which allows to reproduce the observed behaviour [2,4,10] quite accurately. In this continuum model the pedestrians interact by a repulsive (social) force which decays exponentially with the distance between them. This means that in each step of a simulation of N individuals $O(N^2)$ interaction terms have to be evaluated. Furthermore, in complex geometries it occurs quite frequently that two pedestrians are rather close to each other but do not interact since they are separated by a wall. Therefore, in principle, one has to check for all pairs of individuals whether an interaction is possible or not. For large crowds this becomes very time consuming. In contrast, in the model used here pedestrians only interact with the floor field in their immediate neighbourhood. Therefore, one has only $O(N)$ interaction terms. A further advantage is the discreteness of the model which allows for a very efficient implementation for large-scale computer simulations.

We start with a short summary of the models basic concepts.

2. Basic principles of the model

In the model the space is discretised into small cells which can either be empty or occupied by exactly one pedestrian. Each of these pedestrians can move to one of its unoccupied neighbour cells at each discrete time step $t \to t+1$ according to certain transition probabilities (see Fig. 1). The probabilities are given by the interaction with two *floor fields* [6]. These two fields S and D determine the transition probabilities in

[1] Such "learning from nature" is the central idea of a field called *Bionics*.

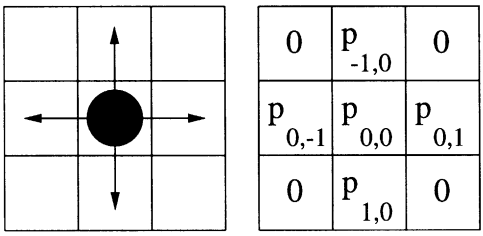

Fig. 1. Allowed motions and the corresponding transition probabilities.

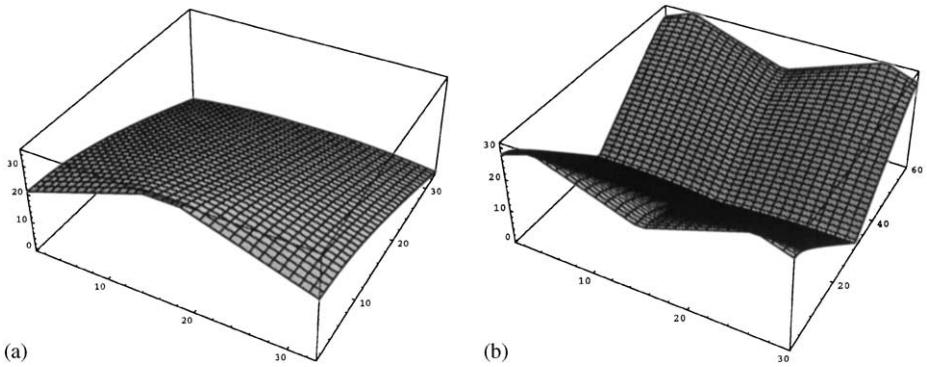

Fig. 2. Static floor field S: (a) for a lattice of size $X \times Y = 33 \times 33$ with one exit of width five cells; (b) lattice of size $X \times Y = 30 \times 60$ and four exits.

such a way that a particle movement is more likely in direction of higher fields. They will be defined in the following subsections where also the basic update rules of the model are summarised.

2.1. The static floor field S

The static floor field S does not evolve with time and is not changed by the presence of the pedestrians. Such a field can be used to specify regions of space which are more attractive, e.g. an emergency exit or shop windows. In case of the evacuation processes considered here, the static floor field describes the shortest distance to a an exit door, lying at the middle of the top wall of the room. Fig. 2 shows graphical representations of S for different geometries. S is calculated due to a certain distance metric for each lattice site so that the field values are increased in the direction to the door. The field values are highest for the door cells. The explicit construction of S can be found in Appendix A.

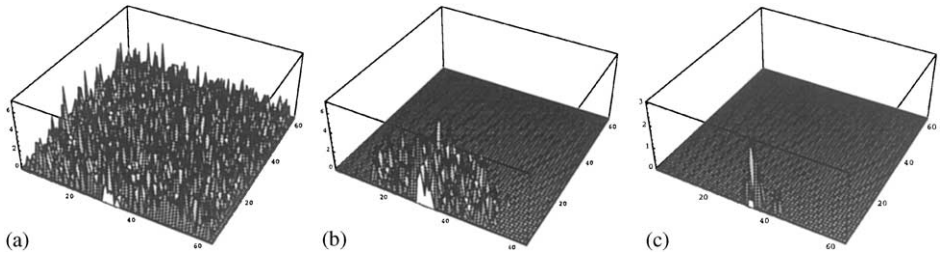

Fig. 3. Dynamic floor field D: (a) beginning evacuation process; (b) middle stages; (c) final stage of evacuation.

2.2. The dynamic floor field D

The dynamic floor field D is a virtual trace left by the pedestrians and has its own dynamics through diffusion and decay. It is used to model an attractive interaction between the particles. Fig. 3 shows three-dimensional plots of D for three stages during evacuation process. At $t = 0$ for all sites (i, j) of the lattice the dynamic field is zero, i.e., $D_{ij} = 0$. Whenever a particle jumps from site (i, j) to one of the neighbouring cells, D of the starting place is increased by one: $D_{ij} \to D_{ij} + 1$.

Therefore D has only non-negative integer values and can be compared to a *bosonic field*,[2] i.e., the bosons dropped by the pedestrians during their movement create the virtual trace. Thus the field value D_{ij} corresponds to D_{ij} bosons. The dynamic floor field is time dependent, it has diffusion and decay controlled by two parameters $\alpha \in [0, 1]$ and $\delta \in [0, 1]$, which means broadening and dilution of the trace. In each time step of the simulation each single boson of the whole dynamic field D decays with probability δ and diffuses with probability α to one of its neighbouring cells. Finally this yields $D = D(t, \delta, \alpha)$.

Note that the dynamic floor field D is only altered by moving particles and therefore it corresponds to a virtual *velocity density* field, rather than a *particle density* field. In Section 3.2 we discuss an alternative definition of the dynamic floor field D as a pure particle density field and its consequences. In the following, we give a short summary of the specific update rules used in the simulations.

2.3. Update rules

The update rules of the full model including the interaction with the floor fields have the following structure [6,11,12]:

(1) The dynamic floor field D is modified according to its diffusion and decay rules (for details, see Section 2.2).

[2] A simplified one-dimensional model with a fermionic field has been used recently for the description of chemotaxis [8].

(2) For each pedestrian, the transition probabilities p_{ij} for a move to an unoccupied neighbour cell (i, j) (see Fig. 1) are determined by the local dynamics and the two floor fields. The values of the fields D and S are weighted with two sensitivity parameters $k_S \in [0, \infty[$ and $k_D \in [0, \infty[$. This yields

$$p_{ij} = N \exp(k_D D_{ij}) \exp(k_S S_{ij})(1 - n_{ij})\xi_{ij} , \tag{1}$$

with

$$\text{occupation number} : n_{ij} = 0, 1 ,$$

$$\text{obstacle number} : \xi_{ij} = \begin{cases} 0 & \text{for forbidden cells, e.g. walls} , \\ 1 & \text{else} , \end{cases}$$

$$\text{normalisation} : N = \left[\sum_{(i,j)} \exp(k_D D_{ij}) \exp(k_S S_{ij})(1 - n_{ij})\xi_{ij} \right]^{-1} .$$

(3) Each pedestrian chooses a target cell based on the transition probabilities p_{ij} determined in the previous step.
(4) The conflicts arising by any two or more pedestrians attempting to move to the same target cell are resolved by a probabilistic method.[3] The pedestrians which are allowed to move execute their step.
(5) D is increased by all moving particles.

The above rules have to be applied to all pedestrians at the same time, i.e., we use parallel update.

Note that we do not use here the so-called *matrix of preference* [6] because it encodes a direction of preferred motion of the pedestrians, which they usually not have at the beginning of an evacuation process. In the following all information about the desired direction of motion is obtained from the floor fields.

In Ref. [6] it has been shown that simple, local update rules for the pedestrians and the two floor fields are sufficient to yield a richness of complex phenomena (see Section 2.4). Obviously this route is superior concerning the computational efficiency and even allows for faster-than-real-time simulations of large crowds [6,14,15], e.g. in evacuation processes in public buildings.

2.4. Collective phenomena

Pedestrian dynamics exhibits are variety of fascinating collective effects [2,4]:

- *Jamming*: At large densities various kinds of jamming phenomena occur, e.g. when many people try to leave a large room at the same time [4,6,10,14–16]. This clogging effect is typical for a bottleneck situation. Other types of jamming occur in the case of counterflow where two groups of pedestrians mutually block each other [17,18].

[3] One can as well solve the arising conflicts using the procedure described in Ref. [6]. It can be shown in [13] that conflicts are important for a correct description of the dynamics.

This happens typically at high densities and when it is not possible to turn around and move back, e.g. when the flow of people is large.

- *Lane formation*: In counterflow, i.e., two groups of people moving in opposite directions, a kind of spontaneous symmetry breaking occurs. The motion of the pedestrians can self-organise in such a way that (dynamically varying) lanes are formed where people move in just one direction [9]. In this way, strong interactions with oncoming pedestrians are reduced and a higher walking speed is possible.
- *Oscillations*: In counterflow at bottlenecks, e.g. doors, one can observe oscillatory changes of the direction of motion [9]. Once a pedestrian is able to pass the bottleneck it becomes easier for others to follow him in the same direction until somebody is able to pass (e.g. through a fluctuation) the bottleneck in the opposite direction.
- *Patterns at intersections*: At intersections various collective patterns of motion can be formed [2,4,19]. A typical example are short-lived roundabouts [2,4] which make the motion more efficient. Even if these are connected with small detours the formation of these patterns can be favourable since they allow for a "smoother" motion.
- *Trail formation*: Although human and animal trails are formed for rather different purposes their structures have some similarities [20,21]. Often human trails are formed as a short-cut which makes it attractive to leave a paved path. Animal trails usually are related to chemotaxis and mark the way to food places.
- *Panics*: In panic situations many counter-intuitive phenomena (e.g. "faster-is-slower" and "freezing-by-heating" effects [22]) can occur. For a thorough discussion we refer to Refs. [4,10] and references therein.

In Refs. [6,14] it has been shown that the new CA model described in the previous subsection is—despite its simplicity—able to reproduce these observed collective effects. This is essential if one intends to use the model for real applications, e.g. the optimisation of evacuation procedures.

3. Evacuation simulations

In the following, we describe results of simulations of a typical situation, i.e., the evacuation of a large room (e.g. in case of fire). At this, we focus on the influence of the sensitivity parameters k_D and k_S on the evacuation times in order to identify the different classes of behaviour exhibited by the model. As we will see interesting collective phenomena between the pedestrians lead to a non-trivial dependence of the evacuation times on K_D and k_S. In Section 3.2 we investigate possible alternative definitions of the dynamical floor field. Section 3.3 is devoted to a simple optimisation problem, namely evacuation from a room with two doors [23].

3.1. The impact of sensitivity parameters

The value of k_S, the coupling to the static field, can be viewed as a measure of the knowledge of the pedestrians about the location of the exit. A large k_S implies a motion to the exit on the shortest possible path. For vanishing k_S, on the other hand, the people will perform a random walk and just find the door by chance. So the case

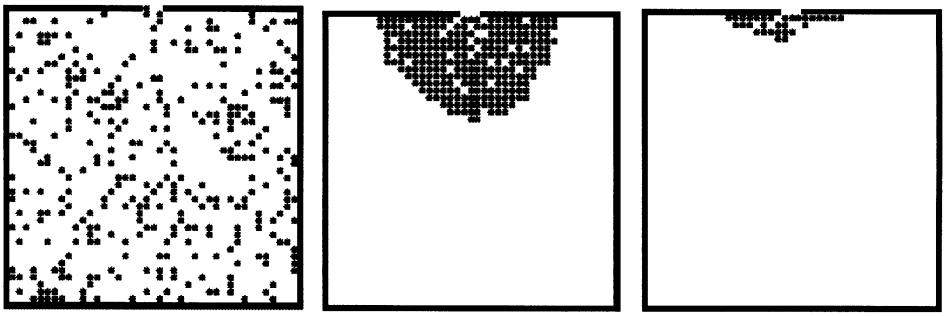

Fig. 4. Typical stages of the dynamics: (a) beginning evacuation ($t = 0$); (b) middle stages; (c) end stage of evacuation with only a few particles left.

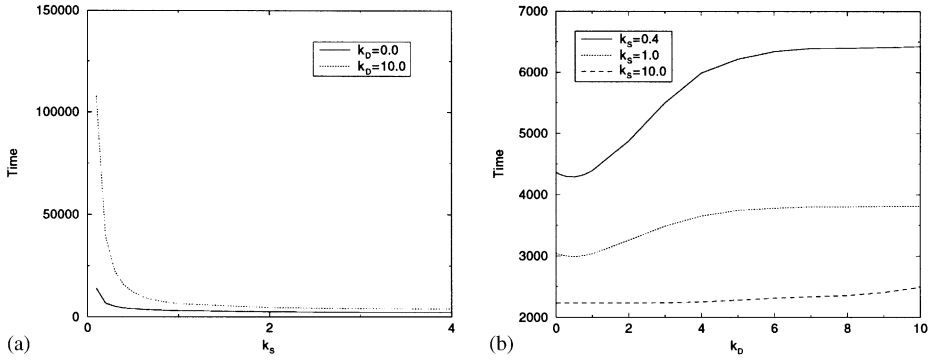

Fig. 5. Averaged evacuation times for a large room (Fig. 4) with an initial particle density of $\rho = 0.3$ and decay constant $\delta = 0.3$: (a) $\alpha = 0.1$ and fixed k_D; and (b) $\alpha = 0.3$ and fixed k_S.

$k_S \ll 1$ is relevant for processes in dark or smoke-filled rooms where people do not have full knowledge about the location of the exit.

The parameter k_D for the coupling to the dynamic field controls the tendency to follow the lead of others. A large value of k_D implies a strong herding behaviour which has been observed the case of panics [10].

We consider a grid of size 63×63 sites with an exit of one cell in the middle of one wall. The particles are initially distributed randomly and try to leave the room. The only information they get is through the floor fields. Fig. 4 shows typical stages of the dynamics for an initial particle density of $\rho = 0.3$, which means 1116 particles. In the middle picture of Fig. 4 a half-circle jamming configuration in front of the door is easy to spot. A typical feature of the dynamics is a radial motion of 'holes' created by particles escaping through the door.

The evacuation times T and their variances σ are averaged over 500 samples and strongly depend on the sensitivity parameters k_D and k_S. Fig. 5(a) shows the evacuation

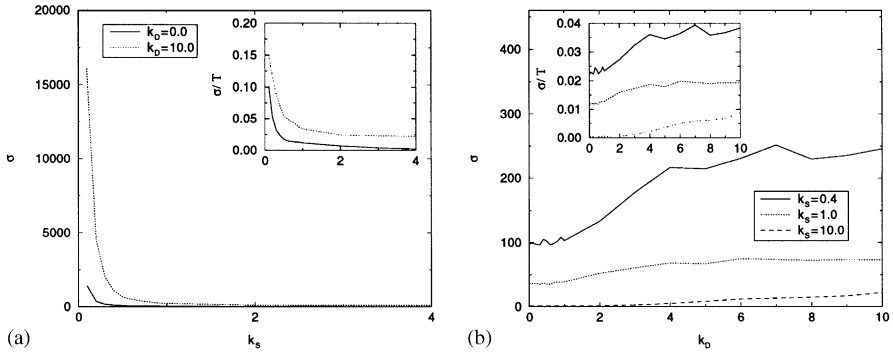

Fig. 6. Averaged variances σ and relative variances σ/T of the evacuation times of Fig. 5: (a) $\delta = 0.3$, $\alpha = 0.1$ and fixed k_D; (b) $\delta = 0.3$, $\alpha = 0.3$ and fixed k_S.

times for fixed sensitivity parameter k_D of the dynamic field and variable sensitivity parameter k_S of the static field and Fig. 5(b) shows the evacuation times for fixed k_D and variable k_S. Fig. 6 shows all corresponding variances σ and relative variances σ/T of the evacuation times of Fig. 5. The averaged evacuation times are always measured in update time steps. With the generic time scale of the model [6,11,12] of about 0.3 s/timestep its easy to translate that into a real time value.

Let us first consider the case of $k_D = 0$, i.e., no coupling to the dynamic field. In Fig. 5(a) one can see the influence of k_S. For $k_S \to 0$ the pedestrians do not sense the strength of the field. Therefore, they do not have any guidance through the surroundings and perform a pure random walk which leads to a maximal value of the evacuation time for $k_S = 0$. For $k_S \to \infty$ they have full information about the shortest distance to the door and the evacuation time converges towards a minimal value. The movement of the particles becomes almost deterministic. Therefore, k_S can be interpreted as some kind of inverse temperature for the degree of information about the inanimate surrounding of the pedestrians.

In the same way the sensitivity parameter k_D of the dynamic field works as an inverse temperature for the information about the virtual trace. If k_S is turned on from zero to infinity, a non-zero value of k_D only means additional noise to the pedestrians and evacuation times increase for higher coupling strength to k_D (see Fig. 5(a)).

Much more interesting is the behaviour for fixed k_S (Fig. 5(b)). The evacuation times saturate at maximal values for growing sensitivity parameter k_D of the dynamic field. The most interesting point is non-monotonic behaviour of $T(k_D)$ with the occurrence of minimal evacuation times for non-vanishing small values of the sensitivity parameter k_D of the dynamic field. Therefore a small interaction with the dynamic field, which is proportional to the velocity density of the particles, represents some sort of minimal intelligence of the pedestrians. They are able to detect regions of higher local flow and minimise their waiting times. This effect is most pronounced for intermediate coupling ($k_S \approx 0.4$) to the static field S, but very weak for strong coupling to S (e.g. $k_S \approx 10$), where the evacuation is dominated by the orientation to the inanimate surrounding. It

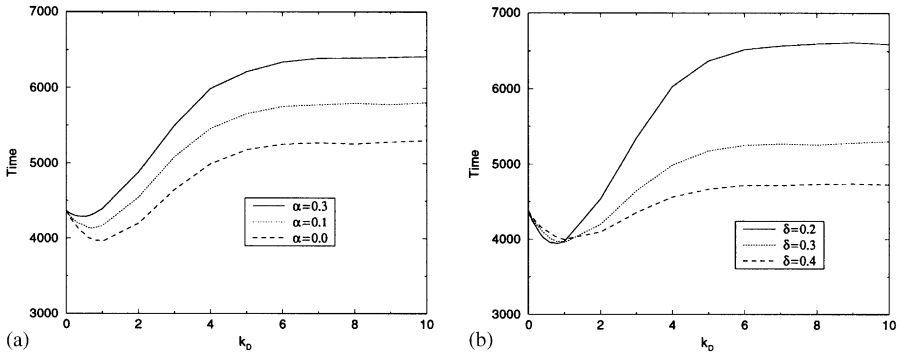

Fig. 7. Averaged evacuation times for a large room for an initial particle density of $\rho = 0.3$: (a) $k_S = 0.4$ and $\delta = 0.3$; (b) $k_S = 0.4$ and $\alpha = 0.0$.

vanishes again for very weak coupling to S ($k_S = 0.1$, not shown in Fig. 5(b)) where the movement of the pedestrians is similar to a random walk.

If the coupling to the dynamic field is further increased, the evacuation times increase again and saturate at maximal values. The interaction with other pedestrians becomes more and more unfavourable similar to the arising of a panic situation. The weaker the coupling to the static field S is, the higher are the evacuation times: the particles than have less information of the inanimate surrounding (for example they cannot find the way to the door because of smoke in a fire situation).

The variances σ of the evacuation times (Fig. 6) show qualitatively the same behaviour as the averaged time values. For strong coupling to S ($k_S \approx 10$, $k_D < 2$) σ tends to zero, which means that the process is nearly deterministic. For weak coupling to S the variance σ increases strongly and also the relative variance σ/T becomes rather large for $k_S \to 0$. From a practical point of view, i.e., evacuations of real buildings, one has to ask whether it makes sense to specify safety just by the average evacuation time alone when (relative) variances can become large. For fixed k_S and varying coupling k_D to the dynamic field the variance σ also behaves qualitatively as T, i.e., it increases with increasing k_D (see Fig. 6(b)).

In the following, we discuss the influence of the decay and diffusion parameters δ and α. In Fig. 7(a) one can see that for $k_S = 0.4$ and a high density of $\rho = 0.3$ the effect of minimal evacuation times for non-vanishing small values of k_D becomes most pronounced in the limit $\alpha \to 0$. Besides that all evacuation times are increased with increasing α. That implies that diffusion of the field only means additional noise and no advantageous information for the particles due to the fast broadening and dilution of the trace for large α.

For decay parameter $\delta \to 0$ the dynamic field persists for a long time and the regime of minimal evacuation times is shifted towards smaller k_D values. Evacuation times for fixed k_D increase monotonically with δ (see Fig. 7(b)). This is a collective effect where the herding behaviour helps to overcome the insufficient knowledge about the location of the exit. In contrast, the evacuation times in the panic regime (i.e., high k_D values)

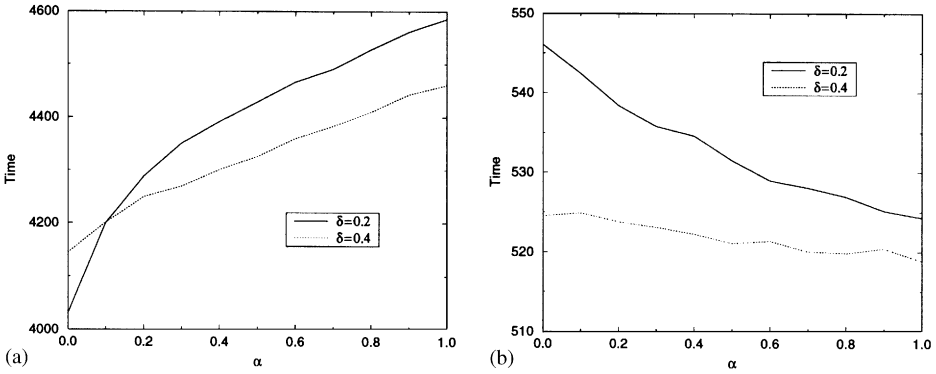

Fig. 8. Averaged evacuation times for a large room (Fig. 4) for two densities, variable α and $k_S = k_D = 0.4$: (a) $\rho = 0.3$, and (b) $\rho = 0.003$.

are increased with smaller δ. With the field values of D the memory of previous steps grows which increases the noise in the system for the particles. Therefore, for large values of k_D a strong herding behaviour would be unfavourable since it tends to 'confuse' the pedestrians which already have a good knowledge about the geometry. This reversed behaviour in comparison with the case $k_D \to 0$ leads to a crossing of the curves in Fig. 7(b). It is interesting to note that this crossing happens in a rather narrow interval around $k_D \approx 1$.

The influence of the diffusion parameter α of the dynamic field in the regime of minimal evacuation times strongly depends on the particle density ρ. As in Figs. 7(a) and 8(a) one can see that in the high density regime an increasing diffusion parameter α always increases the evacuation times for arbitrary decay parameter δ, since the diffusion of the field increases the noise for the particles. In the low density regime one finds the opposite behaviour. Here the diffusion of the dynamic field leads to a higher degree of information for the particles and to favourably long-ranged interactions between them (Fig. 8(b)). For large α the evacuation time increases with decreasing δ whereas for small α one finds just the opposite behaviour. This leads to a crossing of the curves in Fig. 8(a). The main reason is that for larger densities the evacuation time is mostly determined by the clogging which occurs at the exit whereas for small densities clogging is negligible. Furthermore, for small α the traces are rather sharp and so a larger δ just reduces the field strength. In contrast, for large α the traces broaden quickly and are thus diluted such that they form an almost constant background.

Thus three main regimes for the behaviour of the particles can be distinguished. For strong coupling to k_S and very small coupling to k_D we find an *ordered regime* where particles only react to the static floor field and the behaviour than is in some sense deterministic. The *disordered regime*, characterised by strong coupling to k_D and weak coupling to k_S, leads to a maximal value of the evacuation time. The behaviour here is typical for panic situations, e.g. the herding tendency dominates. Between these two regimes an *optimal regime* exists where the combination of interaction with the static and the dynamic floor fields minimises the evacuation time. Here the individuals have

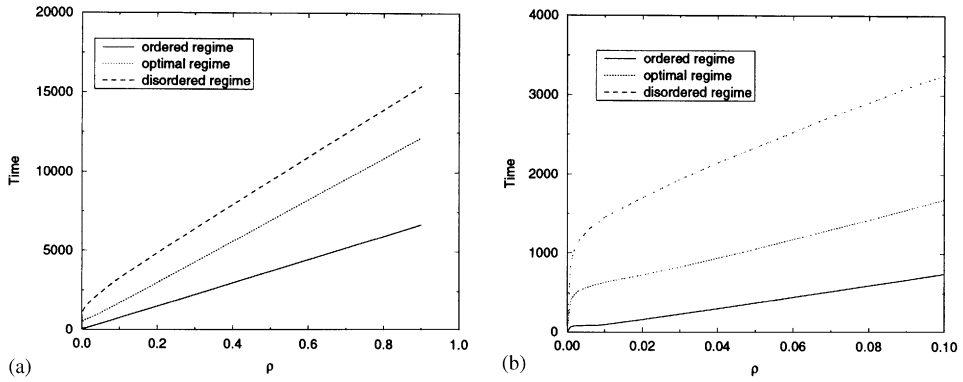

Fig. 9. Average evacuation times for a large room: (a) density regime $\rho \in [0, 0.9]$; (b) more detailed look at the low density regime $\rho \in [0, 0.1]$.

some knowledge about the location of the exits, but through some sort of cooperation the evacuation time T can be optimised.

Fig. 9(a) shows the influence of an increasing particle density for the evacuation times in the three main regimes. For very small densities one finds a very strong increase of the evacuation times with increasing density (Fig. 9(b)). If there are only very few particles in the system, which are distributed randomly over the lattice at $t = 0$, they reach the door nearly independently from each other during the evacuation. Then the evacuation times are nearly proportional to the largest initial distance to the exit. In this regime diffusion of the dynamic field D provides advantageous information to the particles (see Fig. 8(b)). In the density regime $\rho \approx 0.005$ a queue in front of the door begins to form that strongly controls the evacuation time which then increases nearly linearly with growing density due to clogging.

3.2. Alternative definitions of the dynamic floor field

In the following, we want to give a brief discussion of the consequences of several variations and extensions of the definition of the dynamic field D and the corresponding coupling parameter k_D. First we concentrate on the effects of a negative sensitivity parameter $k_D < 0$, corresponding to repulsive interactions between the individuals, on the evacuation times. Fig. 10(a) shows the averaged evacuation times T for a high density of $\rho = 0.3$ and weak coupling $k_S = 0.4$ to the static field for several diffusion parameter values α ($\delta = 0.3$ fixed). For all diffusion parameters α the averaged evacuation time is increasing for decreasing sensitivity parameter $k_D < 0$. This is obvious since the dynamic field D marks the regions of highest flow in the system (e.g. nearby the exit), because of its relation to the velocity density, and therefore an avoidance of this regions should lead to an increased evacuation time. An increasing α value weakens the sharpness of D in the high flow regions and so the effect of the avoidance of this regions is moderated, i.e., the evacuation times decrease for increasing α and $k_D < 0$.

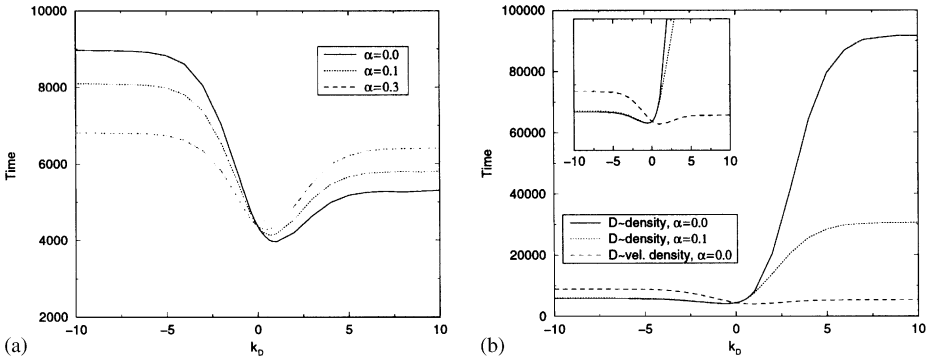

Fig. 10. Averaged evacuation times for variations of D and k_D for a density of $\rho = 0.3$ and a lattice of 63×63 sites: (a) $k_D \in [-10, 10]$ for D proportional to the velocity density; (b) $k_D \in [-10, 10]$ for a field $\tilde{D}$ proportional to the particle density and D proportional to the velocity density.

More subtle consequences arise for the dynamics of the model if the definition of the dynamic field D is changed. Up to now we have considered a dynamic field which is related to the velocity density in the sense that it is only altered by moving particles (see Section 2.2). As an alternative we investigate a field $\tilde{D}$ which is altered by all particles: in each time step each particle increases the dynamic field value of its site by one, i.e., $\tilde{D}$ is proportional to the particle density. Fig. 10(b) shows the evacuation times for fixed coupling strength $k_S = 0.4$ to the static field, variable $k_{\tilde{D}} \in [-10, 10]$ and the two diffusion parameters $\alpha = 0.0$ and $\alpha = 0.1$ for this density field $\tilde{D}$ ($\delta = 0.3$ fixed). As a comparison Fig. 10(b) shows again the corresponding times for the velocity density field D (see Fig. 10(a)) with $\alpha = 0.0$. For positive coupling parameter $k_D > 0$, i.e., attractive interaction, one finds monotonously increasing evacuation times for all diffusion parameters α. The time values for different α begin to branch for $k_D > 1$ such that for $k_D > 5$ the evacuation time for a diffusion parameter $\alpha = 0.0$ is three times higher than for $\alpha = 0.1$. The reason for that becomes obvious from Fig. 11(c) where a two-dimensional visualisation of the density-dependent dynamic field $\tilde{D}$ is shown. The darkest shaded sites correspond to regions of highest $\tilde{D}$ values. Since $\tilde{D}$ is related to the particle density, regions of jamming due to high particle concentration are signified by high $\tilde{D}$ values (e.g. a half-circle jamming in front of a door, see Fig. 11(a)). This effect is strongest for $\alpha = 0.0$, because a non-vanishing diffusion parameter only smoothes the field gradients. Therefore an attractive interaction to such a particle density-dependent field leads to very high evacuation times due to clustering and herding effects known from panic situations, especially for vanishing diffusion of $\tilde{D}$.

For negative sensitivity parameter $k_{\tilde{D}} < 0$, i.e., repulsive interaction, one finds a different behaviour. In the region of $k_{\tilde{D}} \in]-1, 0[$ the evacuation time for the density-dependent field case is minimised. For smaller $k_{\tilde{D}}$ values the evacuation times increase again monotonically. This is similar to the effect of minimised evacuation times for the velocity density related field D and $k_D \in]0, 1[$ (see Fig. 5(b) and inset of Fig. 10(b)). A slight repulsion from regions of high density combined with a weak

Fig. 11. Snapshot of a simulation and the corresponding dynamic floor fields D (for $\alpha = 0$, $\delta = 0.3$): (a) typical middle stage of the dynamics of the original model; (b) the corresponding dynamical field D related to the velocity density; and (c) dynamical field $\tilde{D}$ for a modified model with $\tilde{D}$ related to the particle density.

guidance through the static ground field S ($k_S = 0.4$) should lead to a larger flow and to smaller evacuation times, as well as a slight attraction to regions of high flow (inset of Fig. 10(b)). A strong repulsive behaviour supersedes the directed walk through S and therefore is counterproductive. It leads again to increasing evacuation times. For $k_D < 0$ the evacuation times for the particle density dependent field $\tilde{D}$ are always smaller than for the velocity density dependent field D, since a repulsion from regions of higher particle density should always be more favourable than repulsion from regions of higher flow. However, Fig. 10 indicates that a density-dependent field with repulsive interactions behaves in some aspects as a velocity density dependent field with attractive interactions.

3.3. Room with two doors

As a simple example for safety estimations in architectural planning we investigate how evacuation times change if a gap between two doors is increased from zero to a maximal value. We consider again an ordinary room with no internal structure of grid size 102×102. We start with one door of width two cells in the middle of one wall. Then the door is split into two doors of one cell each separated by gaps ranging from 2 to 98 (Fig. 12(b) and (c)). Fig. 12 shows typical stages of the dynamics for different gap sizes. Averaged evacuation times are measured for all three main regimes introduced in Section 3.1. Depending on the regime, Fig. 13(a) shows a strong influence of the size of the gap for small and for large gaps. In the ordered regime, the evacuation time is almost uninfluenced by the gap size. The reason is the almost deterministic motion of the particles which do not interact with each other through the dynamic floor field D. In the other two regimes, however, the value of the gap can have a large influence due to the strong interaction effects through D. For both the optimal and the disordered regime one finds minimised evacuation times for a wide area of the gap

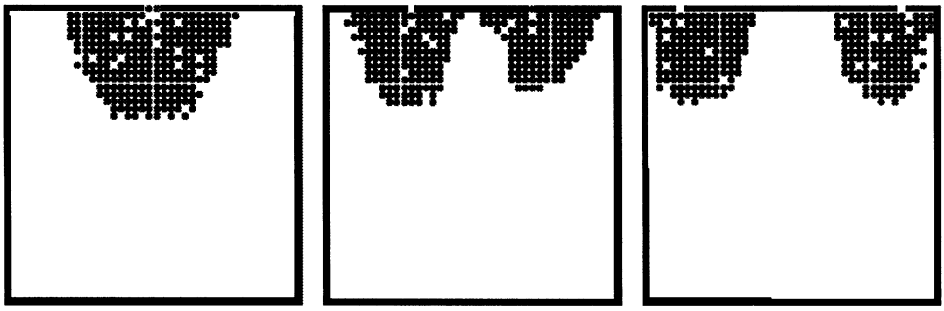

Fig. 12. Typical clogging configurations for a room with two doors: (a) no gap between doors; (b) medium gap size; and (c) doors at the boundaries.

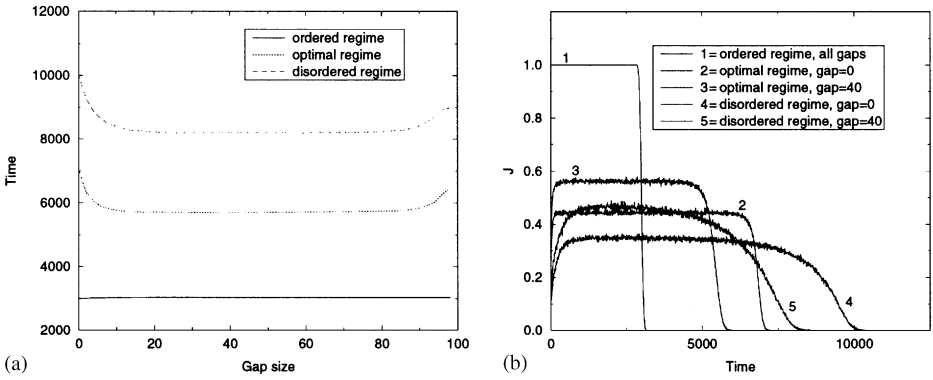

Fig. 13. (a) Evacuation times for all three regimes as function of the gap between doors, and (b) Averaged flows for selected gap sizes for the three regimes.

length ranging from about 20 to 80 cells. For small gaps the evacuation times increase due to the interactions between the pedestrians. For large gaps the presence of the side walls has a negative effect (Fig. 12(c)) and so again the evacuation times increase. For intermediate gaps the crowd of pedestrians will be subdivided into smaller groups (Fig. 12(b)), leading to more favourable interactions between them. This picture is confirmed by the averaged flow values J in Fig. 13(b). A gap size of 40 cells between the doors leads to maximised flow values in the optimal and disordered regime.

4. Conclusions

We have studied simple evacuation processes using a recently introduced stochastic cellular automaton for pedestrian dynamics which implements interactions between

individuals using an idea similar to chemotaxis. Due to its simplicity, the model allows very high simulation speeds and is very well suited for the optimisation of evacuation procedures even in complex situations.

We have focussed on studying evacuation times in a very simple evacuation scenario. The main purpose was to elucidate the influence of the various model parameters, especially of the coupling strengths k_S and k_D to the static and dynamic floor fields, to facilitate their interpretation.

Most important are the coupling parameters k_D and k_S to the dynamic and static floor fields, respectively. k_S is a measure for the knowledge of the individuals about the geometry, especially the location of the exits. For dominating coupling to the static field the pedestrians will choose the nearest exit without much detour. For $k_S \to 0$, on the other hand, they have no knowledge at all and will find the doors just by chance.

The dynamic floor field D is a measure for the velocity density of the pedestrians. The parameter k_D controls the herding behaviour. For dominating coupling to the dynamic field the pedestrians have a strong tendency to follow in the footsteps of others, e.g. because they hope that others have more knowledge about the location of exits. Such a behaviour is relevant for panic situations where this herding tendency becomes important and has been observed empirically [4,10]. In fact, the ratio k_D/k_S has very similar effects as the panic parameter introduced in Ref. [10].

The investigation of alternative definitions of the dynamic floor field has shown that the most realistic results are obtained for the velocity density-dependent field with repulsive interactions as used in the original definition of the model. However, a field related to the particle density with repulsive interactions behaves in some aspects very similarly.

An important result of our investigations is that for achieving optimal evacuation times a proper combination of herding behaviour and use of knowledge about the surrounding is necessary. Then through cooperative behaviour of the individuals evacuation times can be minimised.

We want to emphasise that here only a very simple scenario has been studied in order to identify the different regimes of the model. For realistic applications a procedure to determine the coupling parameters is needed. This work is in progress and results will be published elsewhere [7,13]. In the appendix one possible idea is discussed (see also Ref. [6]). Furthermore, the effects of disorder (e.g. different individuals j having different couplings $k_S^{(j)}$ and $k_D^{(j)}$) are important. Another interesting open question concerns the details of the dynamics of evacuation processes in panic situations. We have assumed, as is also done for the panic parameter in Ref. [10], that the coupling constants do not change during the process. However, in many realistic situations it might be more appropriate to use a panic parameter which increases with time. We leave this important problem for future study.

It is surprising that the properties of the model investigated here are in many respects very similar to the social-force model [9] although the interactions are very different. In our approach pedestrians interact with the velocity-density through an attractive coupling whereas the social-force model uses a repulsive density–density interaction. It would be interesting to get a deeper understanding of these similarities.

Acknowledgements

We like to thank K. Nishinari, C. Burstedde, F. Zielen and D. Helbing for useful discussions.

Appendix A. Construction of the static floor field S

The values S_{ij} for the static floor field for sites (i,j) for the geometries used in this paper can be calculated in the following way: The lattice shall be surrounded by obstacle cells, which are not traversable, except for a number of door cells at $\{(i_{T_1}, j_{T_1}), \ldots, (i_{T_k}, j_{T_k})\}$. The pedestrians can only leave the room through these door cells. The explicit values of S in the examples studied here are then calculated with a distance metric:

$$S_{ij} = \min_{(i_{T_s}, j_{T_s})} \left\{ \max_{(i_l, j_l)} \left\{ \sqrt{(i_{T_s} - i_l)^2 + (j_{T_s} - j_l)^2} \right\} - \sqrt{(i_{T_s} - i)^2 + (j_{T_s} - j)^2} \right\} . \tag{A.1}$$

This means that the strength of the static floor field depends on the shortest distance to an exit. $\max_{(i_l, j_l)}\{\sqrt{(i_{T_s} - i_l)^2 + (j_{T_s} - j_l)^2}\}$, where (i_l, j_l) runs over all cells of the lattice, is the largest distance of any cell to the exit at (i_{T_s}, j_{T_s}). This is just a normalisation so that the field values increase with decreasing distance $\sqrt{(i_{T_s} - i)^2 + (j_{T_s} - j)^2}$ to an exit and is zero for the cell farthest away from the door.

This is only one possible representation of the explicit calculation of the static floor field S. Alternative constructions of S do not change the qualitative results of the investigations, provided that the strength of the static floor field is increased in the direction to the exit [7]. The use of a Manhattan metric is one possible example for a successful construction of S for more complex geometries [7,13].

Once the floor field is specified from the geometry of the problem the coupling constant k_S has to be determined such that a quantitative agreement with experimental data is obtained. Currently, we are investigating different strategies [7,13]. A simple method would be to determine k_S such that the observed velocity and velocity fluctuations of the motion of a single pedestrian are reproduced (see Ref. [6]).

References

[1] D. Chowdhury, L. Santen, A. Schadschneider, Phys. Rep. 329 (2000) 199.
[2] D. Helbing, Rev. Mod. Phys. 73 (2001) 1067.
[3] M. Schreckenberg, S.D. Sharma (Eds.), Pedestrian and Evacuation Dynamics, Springer, Berlin, 2001.
[4] D. Helbing, I. Farkas, P. Molnar, T. Vicsek, in: M. Schreckenberg, S.D. Sharma (Eds.), Pedestrian and Evacuation Dynamics, Springer, Berlin, 2001.
[5] E. Ben-Jacob, Contemp. Phys. 38 (1997) 205.
[6] C. Burstedde, K. Klauck, A. Schadschneider, J. Zittartz, Physica A 295 (2001) 507.
[7] A. Kirchner, Dissertation, Universität zu Köln, 2002; available for download soon at http://www.thp.uni-koeln.de/~aki.
[8] D. Chowdhury, G. Vishwesha, A. Schadschneider, cond-mat/0201207.

[9] D. Helbing, P. Molnar, Phys. Rev. E 51 (1995) 4282.
[10] D. Helbing, I. Farkas, T. Vicsek, Nature 407 (2000) 487.
[11] A. Schadschneider, in: M. Schreckenberg, S.D. Sharma (Eds.), Pedestrian and Evacuation Dynamics, Springer, Berlin, 2001.
[12] A. Schadschneider, Proceedings of "Traffic and Granular Flow '01", Springer, Berlin, 2002.
[13] A. Kirchner, K. Nishinari, A. Schadschneider, in preparation.
[14] C. Burstedde, A. Kirchner, K. Klauck, A. Schadschneider, J. Zittartz, in: M. Schreckenberg, S.D. Sharma (Eds.), Pedestrian and Evacuation Dynamics, Springer, Berlin, 2001.
[15] A. Kirchner, A. Schadschneider, Proceedings of "Traffic and Granular Flow '01", Springer, Berlin, 2002.
[16] Y. Tajima, T. Nagatani, Physica A 292 (2001) 545.
[17] M. Fukui, Y. Ishibashi, J. Phys. Soc. Jpn. 68 (1999) 2861 and 3738.
[18] M. Muramatsu, T. Irie, T. Nagatani, Physica A 267 (1999) 487.
[19] M. Muramatsu, T. Nagatani, Physica A 286 (2000) 377.
[20] D. Helbing, F. Schweitzer, J. Keltsch, P. Molnar, Phys. Rev. E 56 (1997) 2527.
[21] D. Helbing, J. Keltsch, P. Molnar, Nature 388 (1997) 47.
[22] D. Helbing, I. Farkas, T. Vicsek, Phys. Rev. Lett. 84 (2000) 1240.
[23] Java applets for the simulated scenarios can be found at http://www.thp.uni-koeln.de/~as/as.html.